NUKLEONIKA 2006;51(Supplement 1):S49–S54

EPR and ESEEM study of silver clusters in ZK-4 molecular sieves

Jarosław Sadło, Jacek Michalik, Larry Kevan

Abstract Silver clusters generated by γ-irradiation in ZK-4 zeolites – isostructural with Linde type A (LTA) zeolite, have been studied by electron paramagnetic resonance (EPR) spectroscopy. It was shown that even a small decrease of cation capacity resulting from a lower Si/Al ratio in the framework affects distinctly silver agglomeration. In dehydrated ZK-4 with Si/Al = 1.2 and 2.4 only silver dimers are stabilized, whereas in Linde 4A silver hexamers were trapped. In ZK-4 exposed to H_2O and CH_3OH, silver tetramers Ag_4^{3+} efficiently are formed. The results of electron spin echo envelope modulation (ESEEM) showed that the adsorbate molecules are in close vicinity to the clusters. It was postulated that in zeolites with low cation capacity the adsorbate molecules make difficult Ag^0 migration promoting the reactions with Ag^+ cations located in the same sodalite cage.

Key words ZK-4 • EPR • ESEEM • silver clusters

J. Sadło, J. Michalik✉
Department of Radiation Chemistry and Technology,
Institute of Nuclear Chemistry and Technology,
16 Dorodna Str., 03-195 Warsaw, Poland,
Tel.: +48 22 504 1205, Fax: +48 22 811 15 32,
E-mail: esrlab@orange.ichtj.waw.pl

L. Kevan
Department of Chemistry,
University of Houston,
Houston, TX 77204-5641, USA

Received: 6 December 2005
Accepted: 8 February 2006

Introduction

The size-dependent properties of metal nanoclusters are of considerable interest with respect to fundamental knowledge and possible applications in catalysis and nanotechnology. The unique cluster properties originate from size-dependent distribution of electron energy levels and quantum-size effects. For studying the nuclearity of paramagnetic metal clusters, the electron paramagnetic resonance (EPR) specroscopy is a major experimental technique.

Silver exchanged Na-A zeolites with high silver loadings reduced chemically or radiolytically, show unique ability to stabilize paramagnetic silver hexamer – Ag_6^{n+} where $n = 1, 3, 5$ for paramagnetic species [2, 11]. It is postulated that hexameric silver clusters are trapped inside sodalite cages of zeolite A. For smaller silver concentration (up to $1Ag^+$ per unit cell), only silver trimers Ag_3^{2+} were recorded [14]. Silver hexamers were also recorded in irradiated sodalite, but with significantly different spin Hamiltonian parameters [5]. Based on *g* value, the assignment of Ag_6^{5+} is postulated, whereas the hexamer charge in zeolite A should be smaller (1 or 3). It should be noticed that silver hexamers have been never observed in zeolite X or Y, although faujasite structure is also composed of sodalite cages.

In γ-irradiated AgCs-rho zeolite the subsequent formation of Ag^0, Ag_2^+, Ag_3^{2+} and Ag_4^{3+} was observed in thermally annealed samples [7]. Tetrameric cluster is stable above room temperature. After NH_3 adsorption, silver tetramer coordinates six ammonia ligands, two in the first coordination sphere and four in the second one, forming a multicore complex $Ag_4^{3+}(NH_3)_2^{'}(NH_3)_4^{''}$ [12].

Usually, it is possible from the analysis of EPR spectra to deduce the structure of paramagnetic species. However, the resolution of EPR spectra, in general, is too low to record the spectral features from super-hyperfine interactions derived from magnetic nuclei of adsorbate molecules interacting with paramagnetic center. For studying such superhyperfine interaction in polycrystalline media electron spin echo envelope modulation (ESEEM) spectroscopy is best suited. Till now, there are only a few papers available on the interaction of silver clusters with molecular adsorbates in zeolites by the ESEEM method. Based on ESEEM results, it was found that in AgNa-A zeolite silver hexamers, Ag_6^{n+} are only stabilized in those sodalite cages which are surrounded by α-cages not containing H_2O molecules. In contrast, Ag_3^{2+} can be stabilized in β-cage if H_2O molecules are present in close vicinity. In hydrated AgNa-A zeolite trimeric species directly interact with water molecules trapped in the same β-cage [8].

In aluminasilicaphosphate lattice of AgH-SAPO-42, which is isostructural with zeolite A, in dehydrated samples only dimmers Ag_2^+ and trimers Ag_3^{2+} are formed after γ-irradiation. It is due to lower cation capacity in SAPO's lattice in comparison to zeolite A. In the presence of methanol, silver hydroxymethyl radicals are the major paramagnetic products of radiolysis in both A and SAPO frameworks. They are stabilized in α-cages by interaction with methanol molecules [10].

In hydrated and dehydrated AgH-SAPO-5 and AgH-SAPO-11 molecular sieves, Ag^0 atoms produced by γ-irradiation do not form stable cationic silver clusters. However, after exposure to methanol prior to irradiation, silver dimers in SAPO-11 and silver dimers and trimers in SAPO-5 are efficiently formed, as was proved by EPR measurements [4]. Ag_2^+ dimer is located in a 6-ring channel in both frameworks and is stabilized by the interaction with three methanol molecules. Besides, silver clusters and silver hydroxymethyl radicals are also produced. ESEEM results indicate that these radicals are located in 12-ring (SAPO-5) and 10-ring (SAPO-11) channels and are coordinated by two nonequivalent methanol molecules.

The aluminosilicate framework which is isotypic structure with Linde type A (LTA) zeolite, but with Si/Al > 1 are called ZK-4. The preliminary EPR results showed that cationic silver clusters are not stabilized in dehydrated ZK-4 zeolites even for the framework with Si/Al = 1.2 so, only slightly higher than 1 [9]. In contrast, ZK-4 samples exposed to water or methanol stabilized efficiently tetrameric silver clusters. It proves that although geometrical constraints play a crucial role with respect to the nuclearity of stabilized clusters, even small changes in the distribution of framework negative charges are able to affect the silver agglomeration process to a great extent.

For better understanding of the role of sodium cocations and adsorbate molecules on silver clustering process, we studied ZK-4 zeolites with various Si/Al ratio exposed to water and methanol. The nuclearity of silver clusters have been examined by the EPR method and the interaction of silver clusters with adsorbate molecules by ESEEM technique.

Experimental

Na-ZK-4 zeolites with different Si/Al ratios (1.2 and 2.4) were synthesized by a modificed Kerr's method [3]. As the sources of silica and alumina, a colloidal silica sol (Ludox HS40, 40% wt. SiO_2, Dupont) and sodium aluminate (Aldrich) were used, respectively. Tetramethyl-ammonium hydroxide TMAOH (25% TMAOH, Aldrich) was added to the reaction solution as a templating agent. The reaction mixture was placed in a Teflon bottle (or Teflon cap fitted into stainless steel pressure vessel) and heated in an oven at 373 K and autogenous pressure for 2 days. The solid product of synthesis, Na-ZK-4 with TMA template, was filtered and washed with deionized water. After drying at room temperature, it was calcined in O_2 at 813 K for 3 h. The purity and crystallinity of the product were monitored by powder X-ray diffraction (XRD). Si/Al ratios were calculated based on the results of inductive couple plasma (ICP) analysis of calcined samples. Ag^+ cations were loaded into zeolites by cation exchange with $AgNO_3$ solution at room temperature. Silver content in Ag^+ exchanged samples was obtained by ICP as $5Ag^+$ and $4Ag^+$ per unit cell in Na-ZK-4 with Si/Al equal to 1.2 and 2.4, respectively.

After drying, the zeolite samples were loaded into suprasil EPR tubes equipped with stopcocks. Hydrated samples were degassed on a vacuum line at room temperature. Dehydrated samples were heated at 150°C for 2 h and then overnight at 230°C under 600 torr of dry O_2 to reoxidise any reduced silver cations. After removal of oxygen, some samples were exposed to water or methanol vapour at room temperature. Samples selected for ESEEM experiments were exposed to deutered D_2O or CD_3OH and CH_3OD vapours (Cambridge Isotope Laboratories).

All sample were γ-irradiated at 77 K in a ^{60}Co source with a dose of 4 kGy. EPR spectra were recorded with a Bruker ESP-300E X-band spectrometer at various temperatures in the range 110–300 K by using variable-temperature Bruker unit. ESEEM signals were measured with a Bruker ESP-380 FT pulse spectrometer in the temperature range 4.5–6 K using a helium flow cryostat. For three-pulse experiments, a pulse sequence of 90°-τ-90°-*T*-90° was employed and *T* was swept. Simulations of the experimental data were performed using the analytical expressions derived by Dikanov *et al.* [1]. The best fits were found by varying the following parameters: (i) the number of interacting nuclei *N*; (ii) the interaction distance *R* and (iii) the isotropic hyperfine interaction coupling A_{iso}, until the sum of squared residuals was minimized.

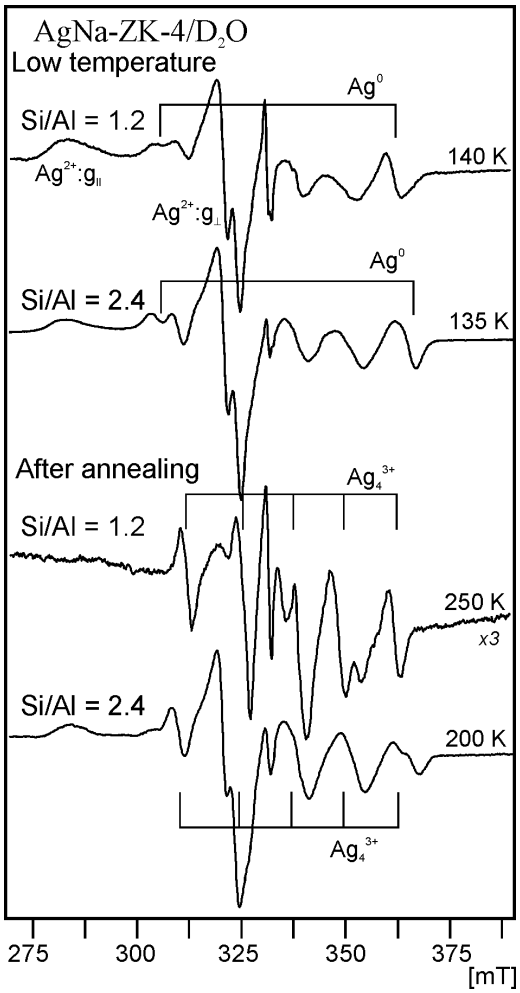

Fig. 1. EPR spectra of AgNa-ZK-4 zeolites with Si/Al = 1.2 and 2.4 exposed to D_2O.

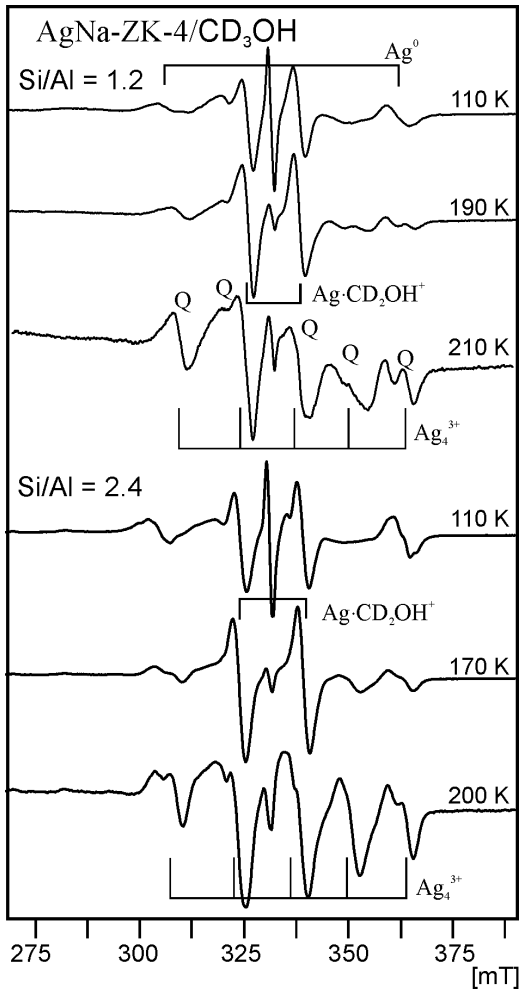

Fig. 2. EPR spectra of AgNa-ZK-4 zeolites with Si/Al = 1.2 and 2.4 exposed to CD_3OH.

Results

EPR results

Dehydrated samples of AgNa-ZK-4 zeolites with Si/Al = 1.2 and 2.4 after γ-irradiation at 77 K show the EPR spectra of silver atoms Ag^0 and divalent silver Ag^{2+}. On thermal annealing to room temperature Ag^0 doublets decay completely in both samples and are replaced by isotropic triplets (A_{iso} = 31.6 mT and g_{iso} = 1.991) of Ag_2^+.

Both Ag^{2+} and Ag^0 species are also the main paramagnetic products of radiolysis at 77 K of AgNa-ZK-4 zeolites exposed to water vapour. However, in this case, thermal treatment leads to the formation of silver tetramers Ag_4^{3+} (A_{iso} = 13.9 mT and g_{iso} = 1.970) for both Si/Al ratios (Fig. 1). It is worthy of noticing that the temperature of Ag_4^{3+} formation depends on the Si/Al ratio. In zeolite with Si/Al = 2.4 the Ag_4^{3+} pentet is easily observed below 135 K, but it decays completely above 230 K. In zeolite with Si/Al = 1.2 the Ag_4^{3+} signal appears only above 140 K and starts decaying above 250 K.

In Ag-ZK-4 samples with methanol vapour adsorbed prior to irradiation, two doublets representing paramagnetic silver species are recorded at low temperature (Fig. 2). The first one with large hyperfine splitting is due to Ag^0 atoms. The EPR parameters depend only slightly on the Si/Al ratio and for zeolites with Si/Al = 1.2 and 1.4 are A_{iso} = 54.6 mT, g_{iso} = 1.989 and A_{iso} = 57.0 mT, g_{iso} = 1.987, respectively. The splittings of the second doublet are much smaller: A_{iso} = 12.2 mT with g_{iso} = 2.003 and A_{iso} = 14.8 mT with g_{iso} = 2.003 for Si/Al = 1.2 and 2.4, respectively. Similar signals were observed earlier in different molecular sieves and were assigned to silver hydroxymethyl radicals $Ag \cdot CH_2OH^+$ having a single σ^1 bond between silver and carbon [6, 13, 15]. The experiments with protonated and deuterated samples proved that spin density is nearly in 100% located on silver and carbon nuclei.

In both types of Ag-ZK-4 zeolites, the signal of silver hydroxymethyl radicals starts decaying above 180 K and at 210 K is not observed at all. In the same temperature range, a new signal *Q* of five lines is gaining its intensity. It was assigned to Ag_4^{3+} cluster with EPR parameters A_{iso} = 12.2 mT with g_{iso} = 1.976 and A_{iso} = 13.5 mT with g_{iso} = 1.976 for Si/Al = 1.2 and 2.4, respectively, slightly smaller than in the Ag-ZK-4/H_2O samples. Ag_4^{3+} signals disappear quickly at room temperature in both types of zeolite samples.

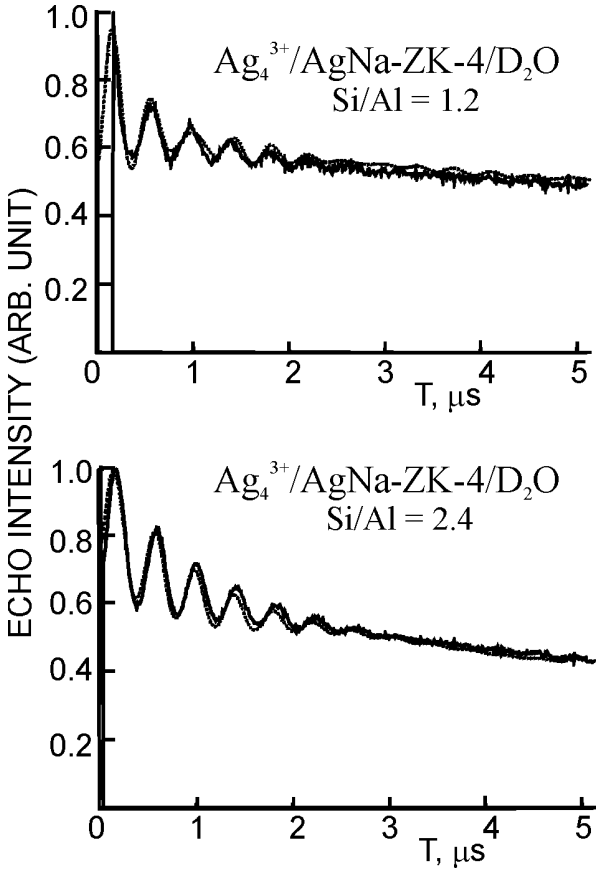

Fig. 3. Experimental (——) and simulated (- - -) three-pulse ESEEM spectra recorded at 6 K of Ag_4^{3+} cluster in ZK-4 zeolites with Si/Al = 1.2 and 2.4 exposed to D_2O.

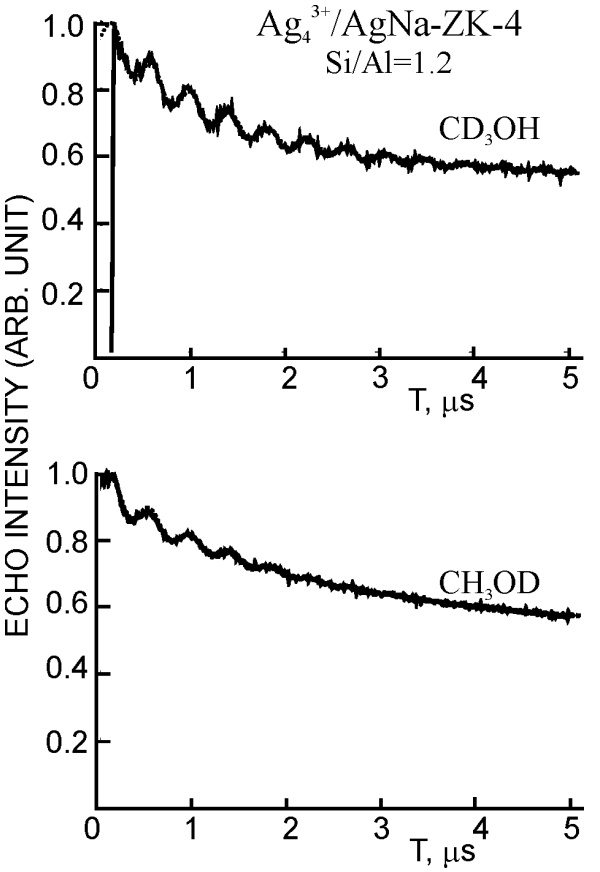

Fig. 4. Experimental (——) and simulated (- - -) three-pulse ESEEM spectra recorded at 6 K of Ag_4^{3+} cluster in ZK-4 zeolites with Si/Al = 1.2 and 2.4 exposed to CD_3OH and CH_3OD.

ESEEM results

For ESEEM study, we used the samples of Ag-ZK-4 exposed to deutered adsorbates, D_2O and methanol with deutered methyl group CD_3OH, and hydroxyl group CH_3OD. The pulse experiments were carried out after sample annealing at 200 K, setting magnetic field at the fourth line of Ag_4^{3+} quintet. Figure 3 shows the deuterium modulation due to the interaction between Ag_4^{3+} cluster and D_2O in Ag-ZK-4/D_2O zeolite. The dashed lines represent the best simulation of ESEEM spectra. The best fits to experimental modulation patterns were obtained assuming the interaction with two deuterons at a distance of 0.265 nm for zeolite with Si/Al = 1.2 and with four more distant deuterons for zeolite with Si/Al = 2.4.

Similar results were obtained for Ag-ZK-4 zeolites with adsorbed methanol (Fig. 4). For the framework with Si/Al = 1.2, Ag_4^{3+} interacts with one methanol molecule and with two methanol molecules in zeolite with Si/Al = 2.4. The parameters of the best simulations for the interaction of Ag_4^{3+} with D_2O and methanol deuterated at methyl and hydroxyl groups are collected in Table 1. A comparison of interaction distances for CD_3OH and CH_3OD clearly indicates that methanol molecules are pointed towards Ag_4^{3+} with their molecular dipoles.

Discussion

ZK-4 zeolite belongs to the *Pm*-3*m* space group with $a = b = c = 1.1919$ nm. Alumina and silica tetrahedra are bonded together to form truncated octahedra called sodalite units or β-cages, with a diameter of 0.66 nm. Four rings of the neighbouring sodalite units are connected by oxygen bridges forming bigger units of

Table 1. The parameters of the best simulations for the interaction of Ag_4^{3+} with D_2O and methanol deuterated in methyl and hydroxyl group

Ag-ZK-4	*N* [atoms]	*R* [nm]	*A* [MHz]
	D_2O		
Si/Al = 1.2	2	0.265	0.23
Si/Al = 1.4	4	0.332	0.025
	CD_3OH		
Si/Al = 1.2	3	0.392	0.02
Si/Al = 1.4	6	0.41	0.04
	CH_3OD		
Si/Al = 1.2	1	0.345	0.03
Si/Al = 1.4	2	0.385	0.01

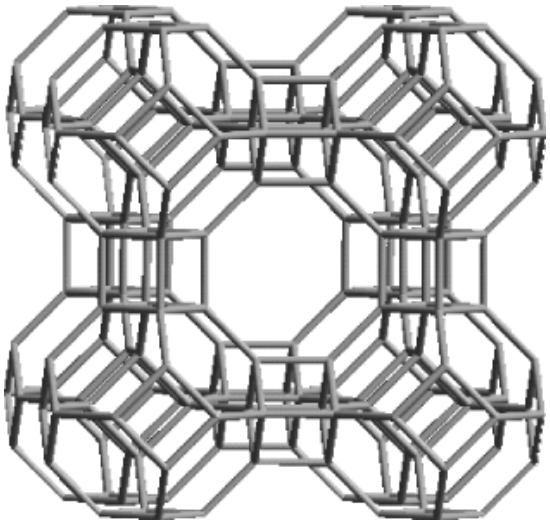

Fig. 5. The framework of Linde type A and ZK-4 zeolites.

26-hedra composed of eight, six and four rings, called α-cages or supercages with a diameter of 1.14 nm. The communication between α- and β-cages is possible only through hexagonal windows with a diameter of 0.23 nm (Fig. 5). The supercages are connected by octagonal windows with a diameter of 0.41 nm.

The cation exchange capacity of zeolite directly depends on the Si/Al ratio. In the LTA zeolite with Si/Al = 1, 12 monovalent cations balance framework negative charges in unit cell. In dehydrated samples of AgNa-LTA zeolite, Ag_6^{n+} clusters are formed in a very broad range of silver loadings, from $2Ag^+$ to $12Ag^+$ cations per unit cell [11].

The ICP data show that in Ag-ZK-4 fully exchanged with Ag^+ the silver loading is $5Ag^+$ and $4Ag^+$ per unit cell for the samples with Si/Al = 1.2 and 2.4, respectively. Despite of that, in dehydrated AgNa-ZK-4 silver hexamers have never been observed for any Ag^+ loadings. In dehydrated samples with Si/Al = 1.2 silver trimers and tetramers appear, while for the framework with Si/Al = 2.4 only dimers are recorded. The above clearly shows that even a small decrease of zeolite cation capacity strongly affects silver clustering in isostructural molecular sieves with similar Ag^+ loading. This might be due to the larger void space in the lattices with larger Si/Al ratio. Under such circumstances, the smaller amount of sodium cocations blocking windows connecting cages and channels makes easier the migration of Ag^+ out of sodalite cages to α-cages or to the surface of crystallites where metallic particles silent for EPR are formed [10].

This conclusion is consistent with the observation of cationic silver clusters of higher nuclearity in hydrated ZK-4 zeolites. For both Si/Al ratios, the intense quintets of Ag_4^{3+} clusters were recorded (Fig. 1). Like Na^+ cocations water molecules facilitate the agglomeration process of silver species located in the same cage by blocking windows of cages. The EPR lines of Ag_4^{3+} are fully developed at 140 K. At that temperature, long-distance migration of silver species, even neutral Ag^0 atoms, does not seem to be possible. However, a short-distance change of cation positions in order to balance more efficiently lattice negative charge in the vicinity of Ag^0 atom formed radiolytically seems quite probable. So, we postulate that Ag_4^{3+} clusters in hydrated ZK-4 zeolites with Si/Al = 1.2 and 2.4 are formed in the β-cages originally loading with four Ag^+. When one Ag^+ is reduced by radiolysis at 77 K the short-distance rearrangement of three remaining cations leads to the formation of Ag_4^{3+} cluster. It seems that silver coalescence process is preferential when the zeolite cages are loaded with Na^+ cocations or H_2O molecules. If the hexagonal windows connecting β- and α-cages are not blocked, then silver atoms are able to escape to bigger cages and Ag_4^{3+} clusters are not formed.

ESEEM results show clearly that water molecules are in close vicinity of radiolytically formed silver tetramers indicating that they play an important role in cluster formation. In ZK-4 zeolite with higher cation capacity (Si/Al = 1.2), silver tetramer interacts with one water molecule. The distance between unpaired electron and deuterium nuclei suggests that Ag_4^{3+} cluster and water molecule are located in the same cage. Possibly, deuterons are placed in the hexagonal window plane with oxygen inside β-cage pointed into tetramer. Other hexagonal windows can be blocked by more distant D_2O molecules non-interacting with Ag_4^{3+}. At 250 K, the trapping site of Ag_4^{3+} becomes ineffective because thermal energy facilitates the molecular movements and Ag_4^{3+} decays.

In contrast, silver tetramers in ZK-4 with Si/Al = 2.4 interact with two water molecules. The interacting distances indicate that water molecules are more distant, possibly with oxygen in the hexagonal window and deuterons in α-cage. We speculate that the interaction with second water molecule is due to the smaller amount of Na^+ cocations in sodalite cages. Then, more water ligands are coordinated by cationic silver species. On the other hand, a lower amount of cations makes the cages more open what facilitates Ag_4^{3+} migration at lower temperature. This results in Ag_4^{3+} decay at lower temperature in ZK-4 with Si/Al = 2.4.

Silver tetramers are also stabilized in ZK-4 zeolites exposed to methanol vapour. However, they are formed at much higher annealing temperature. At low temperatures $Ag{\bullet}CH_2OH^+$ radicals are efficiently formed reducing substantially the amount of silver species that can participate in silver agglomeration. Ag_4^{3+} pentet is appearing in the EPR spectrum only above 200 K. The build-up of pentet is correlated with the decay of $Ag{\bullet}CH_2OH^+$ doublet clearly indicating that agglomeration can proceed only if silver is released from silver hydroxymethyl radicals.

The ESEEM results show that Ag_4^{3+} in the zeolite with Si/Al = 1.2 interacts with one methanol molecule while with two molecules for Si/Al = 2.4. The interacting distances to hydroxyl deuterons of CH_3OD are longer than distances for D_2O molecules. Based on that, we postulate that Ag_4^{3+} cluster trapped in β-cage interacts with one or two methanol molecules located in α-cage and directed with the molecular dipoles into the silver tetramer through the hexagonal window. In the presence of methanol, Ag_4^{3+} clusters are more stable and start decaying only above 280 K. It might be due to the more efficient blocking of lattice windows by more spacious methanol molecules.

The hyperfine splittings of Ag_4^{3+} in ZK-4/CH_3OH differ slightly for samples with different Si/Al ratio. However, additional experiments are necessary to speculate on the effect of cocation loadings on the cluster structure which determines the hyperfine parameters.

That effect was clearly seen for silver hydroxymethyl radicals stabilized in isostructural zeolites with different cation capacity. For example, A_{iso}(Ag) for $Ag \bullet CH_2OH^+$ in zeolite 4A (Si/Al = 1) is 10.6 mT [6, 13, 15] whereas in isostructural SAPO-42 molecular sieve (Si/Al = 5) increases to 13.1 mT. This suggests that sterical constrains can affect the radical structure and subsequently the spin density on silver nucleus which is reflected by the value of hyperfine splitting. To prove that assumption we plan to calculate hyperfine splittings for Ag_4^{3+} cluster and $Ag \bullet CH_2OH^+$ radical stabilized in the traps of different dimensions using density-function theory (DFT).

Conclusions

In contrast to LTA zeolite, which preferentially stabilizes silver hexamers in sodalite cages, the isostructural zeolites ZK-4 with lower cation loadings (Si/Al = 1.2 and 2.4) trapped only clusters with lower nuclearity – dimers in dehydrated samples and tetramers in samples exposed to water and methanol. Those results clearly show that for effective trapping of silver clusters the presence of suitable framework cages is not sufficient. The crucial role plays also total cation capacity and presence of adsorbates which are able to control migration of Ag^0 atoms out of sodalite cages. The ESEEM results proved that water and methanol molecules are in close vicinity of silver clusters in ZK-4 zeolites blocking the migration routes. It was also found that hyperfine splittings of silver clusters depend on total cation capacity. It was speculated that small changes of cluster structure constrained by zeolite lattice and neighbouring cocations might affect the distribution of spin density.

References

1. Dikanov SA, Shubin AA, Parmon VN (1981) Modulation effects in the electron spin echo resulting from hyperfine interaction with a nucleus of an arbitrary spin. J Magn Reson 42:474–487
2. Hermerschmidt D, Haul R (1980) ESR studies on the reduction process of silver zeolites. Bunsen-Ges Phys Chem 84:902–907
3. Kerr GT (1966) Chemistry of crystalline aluminosilicates. II. The synthesis and properties of zeolite ZK-4. Inorg Chem 5:1537–1539
4. Michalik J, Azuma N, Sadło J, Kevan L (1995) Silver agglomeration in SAPO-5 and SAPO-11 molecular sieves. J Phys Chem 99:4679–4686
5. Michalik J, Sadło J, Danilczuk M, Perlińska J, Yamada H (2002) Cationic silver clusters in zeolite rho and sodalites. In: Aiello R, Giordano G, Testa F (eds) Impact of zeolites and other porous materials on the new technologies at the beginning of the new millennium. Elsevier. Studies in Surfaces Science and Catalysis, vol. 142, pp 311–318
6. Michalik J, Sadło J, van der Pol A, Reijerse E (1997) EPR and ESEEM studies on silver hydroxymethyl radicals in molecular sieves. Acta Chem Scand 51:330–333
7. Michalik J, Sadło J, Yu JS, Kevan L (1996) Tetrameric silver clusters in rho zeolite stable above room temperature – ESR studies. Colloids Surf A 115:239–247
8. Michalik J, Wąsowicz T, Sadło J, Reijerse EJ, Kevan L (1996) Pulsed EPR for studying silver clusters. Radiat Phys Chem 47:75–81
9. Michalik J, Yu JS, Sadło J (2000) ESR studies of silver clusters in the isostructural A and ZK-4 molecular sieves. Bull Pol Acad Sci, Chem 48:293–301
10. Michalik J, Zamadics M, Sadło J, Kevan L (1993) Electron spin resonance and electron spin echo modulation studies on radiation-induced silver agglomeration in a SAPO-42 molecular sieve: a comparison with isostructural zeolite A. J Phys Chem 97:10440–10444
11. Morton JR, Preston KF (1986) Paramagnetic silver clusters in γ-irradiated Ag-A molecular sieves. J Magn Reson 68:121–128
12. Sadło J, Danilczuk M, Michalik J (2001) Interaction of tetrameric silver with ammonia in AgCs-rho zeolite. Phys Chem Chem Phys 3:1717–1720
13. van der Pol A, Reijerse EJ, de Boer E, Michalik J (1996) Identification of a silver hydroxymethyl radical in Ag-NaA zeolite using electron spin echo envelope modulation spectroscopy. J Phys Chem 100:3728–3731
14. van der Pol A, Reijerse EJ, de Boer E, Wąsowicz T, Michalik J (1992) The EPR spectrum of Ag_3^{2+}. Mol Phys 75:37–42
15. Wąsowicz T, Mikosz J, Sadło J, Michalik J (1992) Organosilver radicals in gamma-irradiated Ag-NaA zeolite with methanol adsorbate. J Chem Soc Perkin Trans 2:1487–1491